Tolerance analysis versus image quality: a case study for cost-effective space optics

Anees Ahmad, MEMBER SPIE
Chen Feng, MEMBER SPIE
RamaGopal V. Sarepaka*
University of Alabama in Huntsville
Center for Applied Optics
Huntsville, Alabama 35899
E-mail: ahmada@email.uah edu

Abstract. Space optical systems generally require near-theoretical performance in hostile environments within size, weight, and cost constraints. We have addressed the challenge of achieving an optimum image quality through a cost-effective tolerance analysis scheme. Two different space optical systems are considered: the UV imager for the International Solar Terrestrial Physics (ISTP) Mission and an afocal telescope for the Advanced Polarized IR Imaging Sensor (APIRIS). These systems are described along with their required performances and designs. A tolerance study is conducted, and the effect of tolerances on image quality and cost is presented.

Subject terms: space optics, tolerance analysis; image quality; spot diagrams, cost considerations

Optical Engineering 34(2), 575–583 (February 1995).

1 Introduction

The major goal in the development of a space optical system is to achieve the required image quality within the physical and cost constraints. A number of critical steps are involved between the design stage and its cost-effective realization. Many designs appear excellent on paper but are impractical to manufacture or cost too much. This gap between the design and hardware can be bridged only by practical tolerancing. Apart from achieving the required image quality, intelligent tolerancing can also reduce the cost considerably. System requirements for space optics are very exacting, often reaching near-theoretical limits. To our knowledge, no standard guidelines on tolerance studies[1] for space optics are available Due to shrinking budgets and ever-growing demands on the image quality, a fresh look is necessary to explore the tolerancing for this special class of optical systems.

2 System Descriptions

In this study, two generic space optical systems are considered: the UV imager for International Solar Terrestrial Physics (ISTP) Mission[2] and an afocal telescope for the Advanced Polarized IR Imaging Sensor (APIRIS). The UV imager is an all-reflective system with off-axis higher-order aspheric reflecting surfaces operating in the UV region. The afocal telescope of APIRIS is a rotationally symmetric catadioptric system operating in the IR region.

2.1 *UV Imager: System Specifications*

The UV imager has been selected for its complexity. It covers a large field without any image intensity loss due to obscuration or vignetting. The design requirements for the UV imager are (1) simultaneous coherent imaging over the spectral range 130 to 190 nm; (2) field of view 8 deg; (3) angular resolution 0.6 mrad, corresponding to 30-km spatial resolution at altitudes between 6 and 9 earth radii; (4) scattered light less than 10% of incident beam; (5) module size $229 \times 203 \times 203$ mm ($9 \times 8 \times 8$ in.); (6) f number 2.9; (7) focal length 125 mm.

2.2 *UV Imager: Optical Design*

A three-mirror (primary, secondary, and tertiary mirrors) off-axis optical configuration (Fig. 1) was selected for imaging over the entire spectral range with varying intensity conditions. This configuration provides an obscuration-free aperture and an achromatic image quality. The mirrors are conic sections with higher order aspheric constants. These were designed around a common optical axis for an easy alignment. The pupil was located eccentrically to eliminate the obscuration and vignetting. This also helped in locating the field stop and baffles, thereby minimizing the scattered light. The primary and secondary mirrors form an intermediate image, and the tertiary mirror relays it to the final image plane. The spot diagrams for 8 deg of field were presented previously.[2]

2.3 *UV Imager: Optomechanical Design and Fabrication*

The objective of the optomechanical design of the UV imager was to achieve long-term stability at minimum fabrication cost. The design of the mirror mounts was kept very simple to facilitate the assembly, alignment, and testing of the system. The required machining tolerances for the mounts could

*Currently on an Indo-U S science and technology fellowship from Central Scientific Instruments Organisation, Chandigarh India

Paper 29064 received June 27, 1994; revised manuscript received Sep 24, 1994; accepted for publication Sep 26, 1994 This paper is a revision of a paper presented at the SPIE conference on Current Developments in Optical Design and Optical Engineering IV, July 1994, San Diego, Calif The paper presented there appears (unrefereed) in SPIE Proceedings Vol 2263

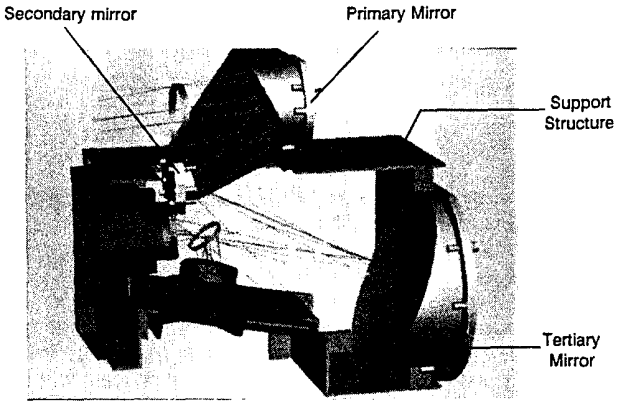

Fig. 1 Three-dimensional model of UV imager.

be achieved by fairly conventional machining methods, since precision shims were employed during the final assembly.

The mirrors were fabricated from 6061-T651 aluminum alloy. On each mirror, reference surfaces were provided for metrology and alignment purposes. The mirrors were rough diamond machined close to the desired aspheric surfaces and were electroless nickel plated on both sides to minimize bimetallic effects. Final optical surfaces were achieved by single-point diamond turning. Later, the mirrors were post-polished to achieve a surface finish of better than 20 Å rms to conform to the 10% scattering limitation. The optical bench of the UV imager was fabricated from magnesium to minimize its weight. Moreover, the coefficient of thermal expansion of magnesium is compatible with that of the aluminum alloy used for the mirrors. Each mirror was mounted to the optical bench using a special alignment fixture, and the desired axial spacings were achieved by using precision-machined shims between the mirrors and optical bench.

2.4 *Afocal Telescope for APIRIS*

The afocal telescope is a rotationally symmetric system employing refractive and reflective elements. Its performance requirements are (1) operational spectral range 8 to 12 μm; (2) afocal magnification 7; (3) field of view 4.77 deg; (4) output beam diameter 11 mm (0.43 in.); (5) output beam to be coupled to a pair of scanning mirrors separated by 20 mm (0.8 in.); (6) resolution in a rectangular field 64×40 pixels; (7) module size 267×254×152 mm^3 (10.5×10×6 $in.^3$). Due to space constraints and to minimize the cost of lenses, a folded configuration was selected in place of an in-line configuration.

2.5 *Afocal Telescope: Optical Design*

SYNOPSYS software was used to design and analyze the performance of the afocal telescope. Figure 2 shows the telescope layout for a 76-mm (3-in.) exit-pupil distance. The results were also verified by CODE V program. In the final design, the surface radii were chosen to match those of available manufacturing tools Germanium lenses and aluminum coated Zerodur fold mirrors were used to minimize the transmission losses. The point spread function plots (Fig. 3) and spot diagrams (Fig. 4) were generated by backward ray tracing. The performance is shown in the object space. The

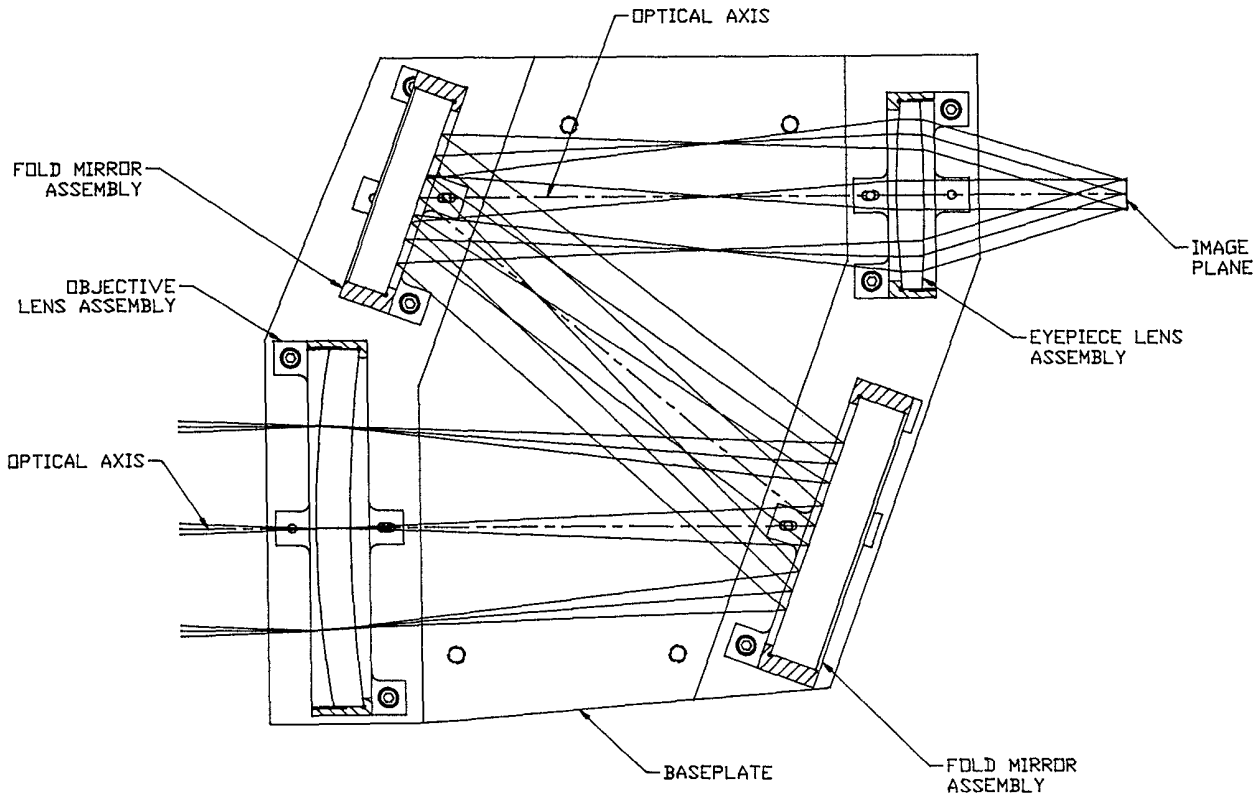

Fig. 2 Sectional view of afocal telescope showing ray trace and optical mounts

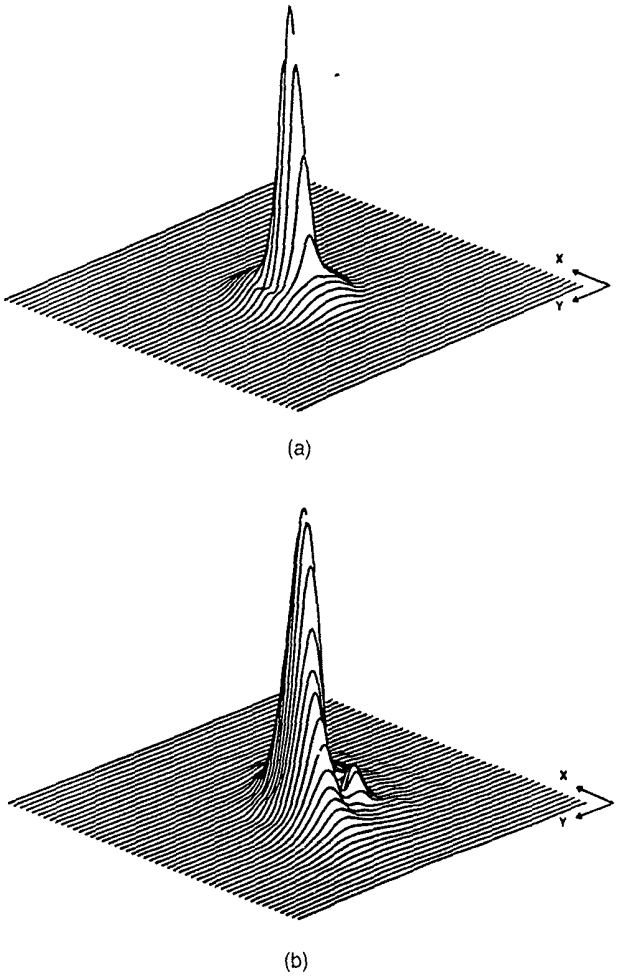

Fig. 3 Point spread function with scanner at (a) neutral and (b) extreme positions for afocal telescope Airy-disk radius 0 00016 rad

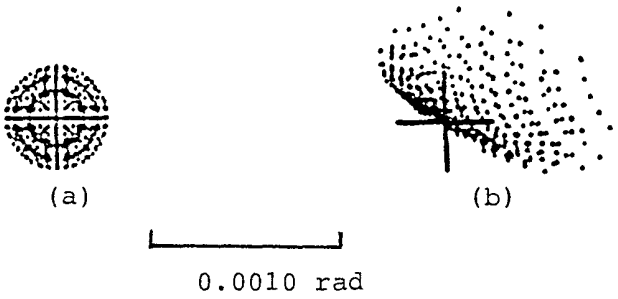

Fig. 4 Spot diagram with the scanner at (a) neutral and (b) extreme positions for afocal telescope

point spread function plots show that the system has near-diffraction-limited performance, and the spot diagrams show that the image quality satisfies the resolution requirements.

2.6 *Afocal Telescope. Optomechanical Design and Fabrication*

Simple lens and mirror mounts with precision bores were designed to achieve the required centration and tilt alignment Relative axial alignment between the optical elements was ensured by providing two precision pins for each of the mounts. These pins were installed into the baseplate in one machining setup. The mounts and base plate were black anodized to minimize scattering losses. The lens surface roughnesses were less than 20 Å rms as measured by a WYKO interferometer. The mirrors had a figure better than one-tenth wave at 632.8 nm and a surface roughness better than 10 Å rms. The lenses and mirrors were bonded into their mounts with a suitable low-expansion (11.4×10^{-5} ppm/°F) and low-shrink (0.8%) room-temperature vulcanizing (RTV) adhesive.

3 Tolerance Study and Cost Analysis

3.1 *Image Criteria*

In any optical tolerance analysis, the study of image degradation with parameter variation is of primary concern. Earlier as well as the recent tolerancing schemes are based on transverse ray aberrations and the modulation transfer function (MTF).[3,4] Sometimes the MTF alone may not represent the full capabilities and limitations of an optical system under perturbation. In this investigation, the average rms spot size (taken at the center and four extreme points of the field) was used as a measure of image degradation due to parameter variation.

3.2 *Tolerancing Scheme*

Since space optical systems are designed to perform over specific wavelength ranges, only space-qualified glasses are chosen, and tolerancing of glass characteristics is not necessary. The cosmetic defects of the optical elements were not considered in this study. Also, the systems were designed to have a reasonable diameter-to-thickness ratio for cost reasons. In this paper, the cost effect of such invarying parameters is not presented. This study focuses on the relative parameter sensitivity and the resultant cost increase. Presently available commercial optical design codes offer routine tolerancing schemes. For the space optical systems under study, the tolerance analysis is situation and need based, so a standard three-step tolerancing process[5] is adopted in this study. Also, this tolerancing procedure explores the reoptimization of axial spacings (except in folded configuration) in order to compensate for the variations in rms spot size due to changes in other design parameters.

Initially, each parameter was varied independently and the resultant systems were evaluated. The allowable parameter variations were determined for certain percentages of rms spot expansion. In the second step, the parameters were varied simultaneously within their respective limits corresponding to different spot expansions. A statistical method was used to change each parameter randomly (within its range) and to form a series of multiple systems. Next, the average rms spot sizes of the systems in each series were computed. The systems were then sorted on an rms spot expansion criterion to determine their acceptance or rejection percentage. This approach provides realistic tolerance data

For a zero-tolerance system, the cost to produce a required mechanical or optical dimension reaches infinity. On the other hand, if any and all tolerances are allowed, the cost to produce a required dimension will constitute some base cost that in-

cludes the material, infrastructure, and labor required. Tolerances of an optical system have an interesting effect on the cost increase above the base cost. The cost is inversely proportional to tolerance, and no two tolerances have the same cost effect. The cost analysis in this study incorporated these factors.[6] The contribution to the overall cost due to the tolerance of the i'th parameter is given as

$$\$_i = A_i/T_i + B_i \ ,$$

where T_i is the tolerance function with an empirical parameter-based constant A_i, and B_i is the base cost. The base cost includes typically the generating cost, part setup cost, cost of grinding and polishing, and cost of centering and edging. Part of this cost is independent of component tolerance. In this study, the base cost of an optical element was taken as 100. However, this base cost is parameter and system dependent, and hence cannot be compared for different parameters and systems. In this tolerance-cost analysis, the empirical equations used to determine the cost versus tolerance are those generally used by the optical industry.[6,7] They are based on the most common facilities and skills available in optical shops. Using them, the cost profiles for different parameters are evaluated for different rms spot size expansions.

3.3 *Tolerance Study for UV Imager*

The UV imager has three higher order off-axis aspheric mirrors. In this study, it was observed that the higher order aspheric-term variations of these mirrors did not contribute notably to the rms spot size expansion in relation to the curvature, and that the surface figure error could be modeled by the square term alone. Therefore, the surface figure and the curvature variations were evaluated in terms of maximum surface sag variations.

The mirrors (primary, secondary, and tertiary) were nonaxisymmetric. Therefore, their displacements were studied in all six degrees of freedom: three axes of translation (decenters along the X and Y axes in a plane normal to the page, and the axial shift along the optical axis Z) and three tilts (tilts about the X and Y axes, and rotation about the optical axis). Corresponding average rms image spot size expansions were evaluated. These expansions were not symmetrical with parameter variation, due to the nonaxisymmetry of the mirrors. The parametric variations (along the horizontal axis) and spot expansions (along the vertical axis) are plotted in Figs. 5 through 11. In these figures, PM denotes primary mirror, SM denotes secondary mirror, TM denotes tertiary mirror, and the 10% dashed line corresponds to a 10% expansion of rms spot size. In all plots, the starting system was the best compromise between the required image quality and other design constraints. Therefore, potential rms spot reductions apparent in isolated cases of the parametric variations did not necessarily result in an acceptable system. For example, a change (between 0 and -0.0035 mm) in the shape of the primary mirror will result in a smaller spot size (see Fig. 5), but also leads to a impractical system. It was also seen that the modeled variations of some parameters (e.g., sag variation of the secondary mirror, X decenter of the secondary and tertiary mirrors) did not result in 10% expansion of the spot size. This does not mean that an infinite variation of these parameters could be tolerated. Therefore, some practical limiting values were assigned to them.

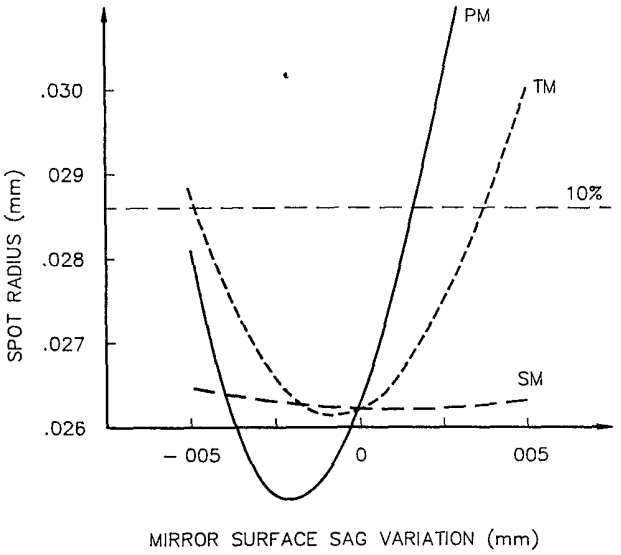

Fig. 5 Spot size expansion with mirror surface sag for UV imager.

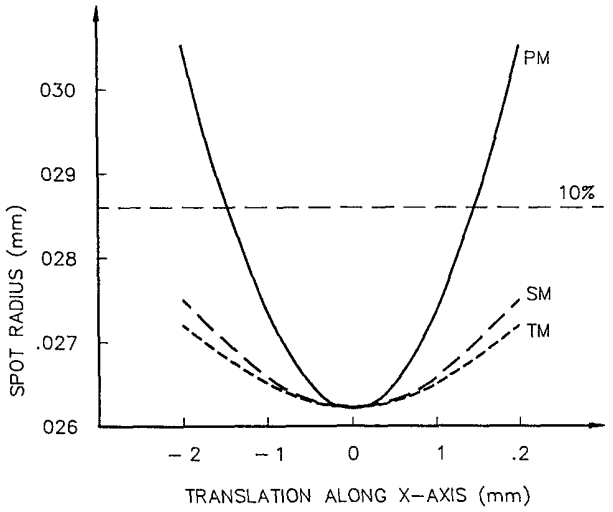

Fig. 6 Spot size expansion with mirror X decenter for UV imager.

So far, the parameters have been systematically varied, one at a time, but in a practical system, no variation can be independent. On the other hand, the result of simultaneous variation of the parameters up to their maximum allowable tolerance values would be disastrous. Therefore, the tolerances were graded into ranges of one-third, one-half, and two-thirds their maximum allowable values. Table 1 lists the sensitivities of the system parameters thus obtained from these plots (Figs. 5–11). In this table, the maximum allowable tolerance values correspond to 10% rms spot size expansion. The other three columns correspond to 33%, 50%, and 67% ranges of these values. The tilts and rotation for each mirror were converted into linear units using the distances between the mounting screws. Table 2 represents the accuracies of the mirrors achievable by a typical diamond turning CNC machine without requiring any special calibration and setup. Some of the required sensitivities (in Table 1) were impractical to achieve on this CNC machine.

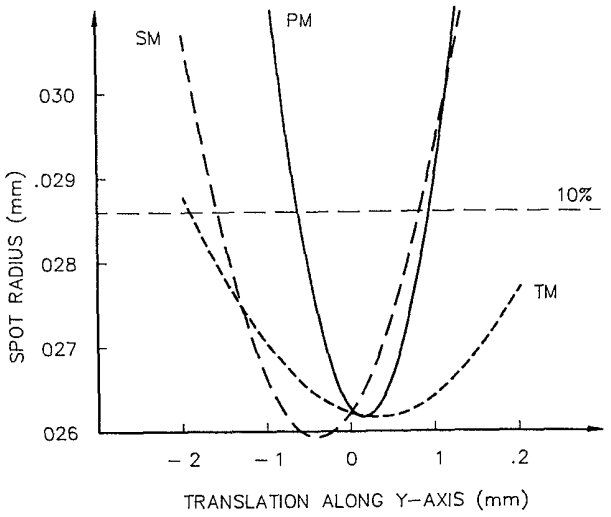

Fig. 7 Spot size expansion with mirror *Y* decenter for UV imager

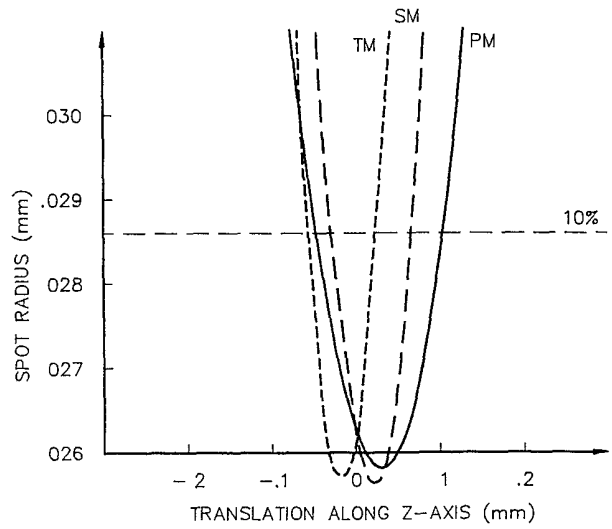

Fig. 8 Spot size expansion with mirror axial shift for UV imager

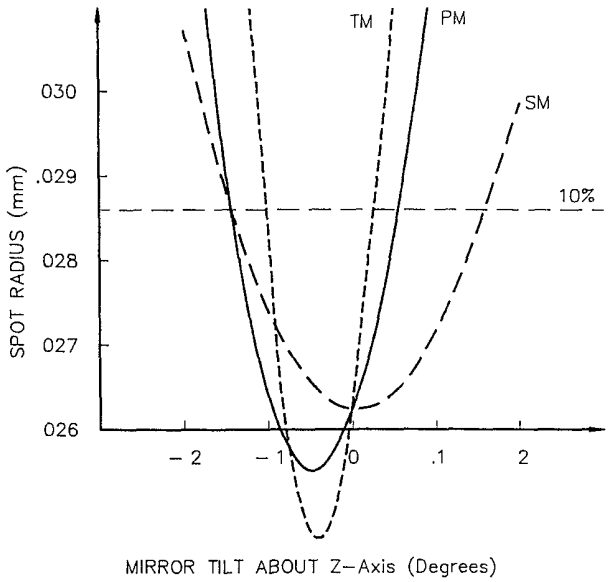

Fig. 9 Spot size expansion with mirror tilt about optical axis for UV imager

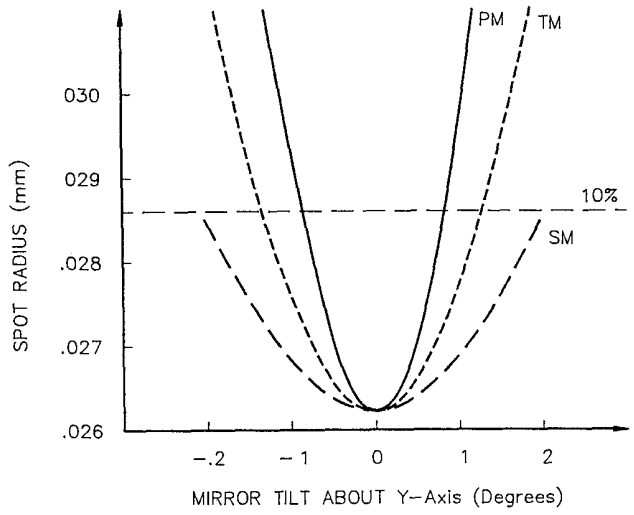

Fig. 10 Spot size expansion with mirror tilt about *Y* axis for UV imager.

Next, the parameters were simultaneously and randomly varied within each of the 33%, 50%, and 67% limits. A statistical code was written and used for this purpose. Thus, three groups of systems (with 100 systems in each set) were formed. For example, the maximum allowable sag tolerance value of the secondary mirrors was 0.01 mm (Table 1). Then in the first set (33% group) of systems, it was allowed to vary up to 0.0033 mm along with the corresponding values of other parameters. In the second set (50% group), it was varied up to 0.005 mm, and in the third set (67% group), its limit was 0.0067 mm.

In the third stage, all these systems were analyzed for image intensity distribution. The systems were then sorted on a criterion of 10%, 20%, 30%, and 40% spot size expansion. Figure 12 shows plots of the percentage of successful systems versus rms spot expansion for the three ranges of parameter variations. It can be seen that the number of systems (out of 100 generated in each group) conforming to 10% rms spot expansion was (1) 93 for the 33% group, (2) 78 for the 50% group, and (3) 60 for the 67% group. The corresponding probability values for systems for a 20% rms spot expansion were 96, 91, and 80. As expected, tight tolerances resulted in a larger number of systems meeting a higher image quality criterion.

Finally, the tolerance values obtained from the individual variation study were translated into cost terms using the standard cost analysis methods.[6,7] Table 3 gives the resulting parameter tolerances versus cost. Figures 13–15 show plots of the parameter tolerances versus the relative cost for the primary, secondary, and tertiary mirrors of the UV imager. It is seen that for tight individual tolerances, the cost is higher Axial shift and surface sag errors are greater contributors to the cost than the other parameters Therefore, cost can be significantly reduced by specifying looser tolerances for sags

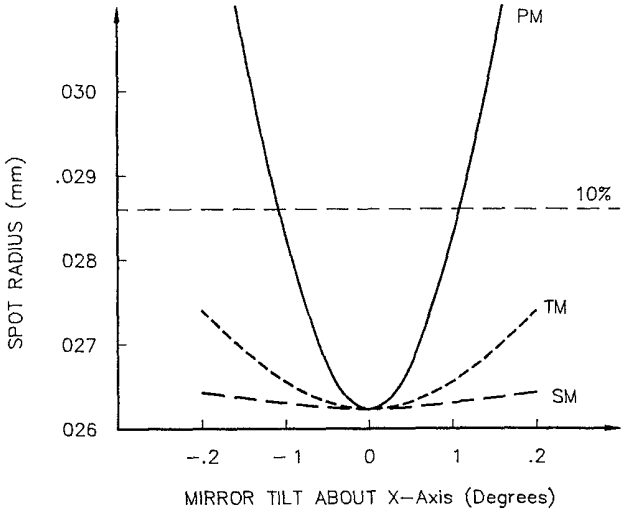

Fig. 11 Spot size expansion with mirror tilt about *X* axis for UV imager

and axial spacings, and tighter tolerances for the other parameters.

3.4 *Tolerance Study for Afocal Telescope*

The afocal telescope for APIRIS is rotationally symmetric and conforms to normal tolerancing procedures used by commercial programs. SYNOPSYS software was used for the tolerance study of this system. As in the UV imager, inititally each parameter was varied independently and the maximum allowable limits of all parameters corresponding to 10%, 15%, 20%, 25%, 30%, 35%, and 41% spot size expansions were determined. Then, all parameters were randomly and simultaneously varied within these tolerance limits. The systems thus obtained were evaluated for their rms spot size expansions for a 2σ confidence (97.7% acceptance level) to determine their acceptance levels. Table 4 gives the tolerances thus obtained for 41%, 30%, 20%, and 10% spot size expansions for the objective and eyepiece of the afocal telescope. Finally, the cost profiles of these tolerances were analyzed by standard methods.[6,7] Table 5 gives the cost escalation for the individual tolerances. Figures 16 and 17 show

Table 2 Tilts and rotation accuracies of UV imager mirrors achievable by a typical CNC diamond turning machine (dimensions are in degrees)

Primary mirror	Machining Measurement Total	0057 0286 ≃ 029
Secondary mirror	Machining Measurement Total	0115 0573 ≃ 057
Tertiary mirror	Machining Measurement Total	0029 0143 ≃ 014

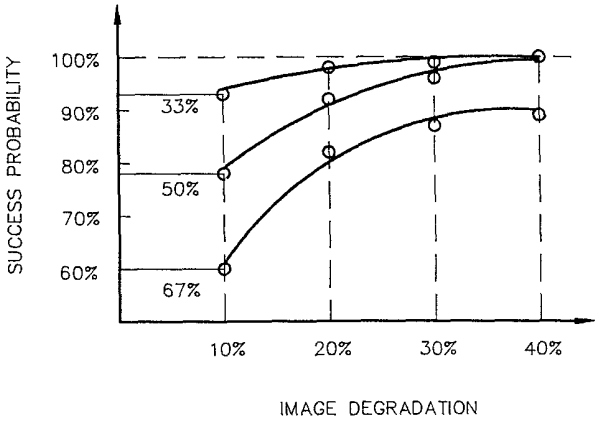

Fig. 12 System success probability with image degradation for 33%, 50%, and 67% maximum allowed tolerances for UV imager

Table 1 UV imager mirror sensitivities for 10% expansion of rms spot (dimensions are in mm, PM: primary mirror; SM: secondary mirror; TM tertiary mirror, tilts are converted into linear units)

		Maximum allowable tolerance values	33% of maximum tolerance values	50% of maximum tolerance values	67% of maximum tolerance values
Surface sag error	PM	0035	0012	0018	0023
	SM	0100	0033	0050	0067
	TM	0043	0014	0022	0029
X - Decenter	PM	145	048	073	097
	SM	280	090	140	190
	TM	344	115	172	229
Y - Decenter	PM	080	027	040	054
	SM	122	041	061	081
	TM	220	073	110	147
Axial shift	PM	076	025	038	051
	SM	040	013	020	027
	TM	046	015	023	031
Tilt along X-axis	PM	0436	0144	0218	0292
	SM	0336	0111	0168	0225
	TM	0567	0187	0284	0380
Tilt along Y-axis	PM	0867	0286	0433	0581
	SM	0959	0317	0480	0643
	TM	2719	0897	1359	1822
Rotation along Z-axis	PM	0977	0323	0489	0655
	SM	2002	0661	1001	1342
	TM	5540	1828	2770	3712

Table 3 UV imager parameter tolerances versus cost escalation for 10% expansion of rms spot (**. beyond the accuracy of a typical CNC machine, base cost = 100)

		Relative Cost			
		Maximum Tolerance	67% Tolerance	50% Tolerance	35% Tolerance
Surface sag error	PM	109 07	113 80	117 64	**
	SM	103 18	104 74	106 35	109 62
	TM	107 39	110 95	114 43	122 68
X-Decenter	PM	102 19	103 27	104 35	106 61
	SM	101 13	101 67	102 27	103 53
	TM	100 92	101 39	101 85	102 76
Y-Decenter	PM	103 97	105 88	107 94	111 76
	SM	102 60	103 92	105 20	107 74
	TM	101 44	102 16	102 89	104 35
Axial shift	PM	104 18	106 23	108 36	112 70
	SM	107 94	111 76	115 88	124 42
	TM	106 90	110 24	113 80	121 17
Tilt (along X-axis)	PM	102 91	104 35	105 83	108 82
	SM	103 78	105 64	107 56	**
	TM	102 24	103 34	104 47	106 79
Tilt (along Y-axis)	PM	101 46	102 16	102 93	**
	SM	101 32	101 98	102 65	104 01
	TM	100 47	100 70	100 93	101 42
Rotation along Z-axis	PM	101 30	101 94	102 60	103 93
	SM	100 63	100 95	101 27	101 92
	TM	100 23	100 34	100 45	100 69

plots of tolerance sensitivity in terms of cost versus image quality for the objective and eyepiece. It can be seen that the tolerance of the radius of curvature is most cost sensitive. Lens decenters appear to have less effect on cost and image quality. Compared to the radius of curvature's effect on image degradation and cost, the surface figure, wedge, and thickness tolerances have moderate effect.

4 Conclusions

A cost analysis has been presented for two different space optical systems, based on a criterion of tolerance versus rms spot expansion. It should be noted that the relative-cost numbers presented are system specific and cannot be correlated for two different systems. Since space optics are not mass produced, selective assembly methods cannot be employed to choose the best parts. Therefore, the cost of space optics is higher than that of commerical optical systems. This higher cost is due to many factors, including space-qualified glasses, special tools for fabrication, and stringent testing procedures. Also, the fabrication and assembly tolerances add to the cost. It is observed that, of all the fabrication parameters, the radii of curvature are the largest single contributors to the rms spot expansion and cost. Another point of interest is the relative cost of optical and mechanical sensitivities. It is observed that in some cases the required accuracies and image quality can be inexpensively obtained by smart optomechanical design.

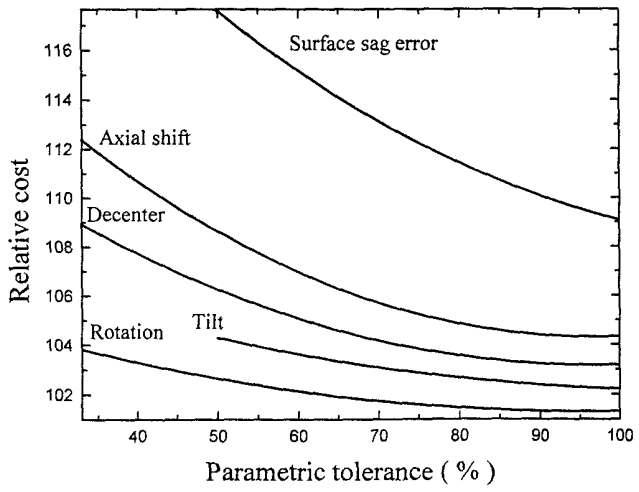

Fig. 13 Parameter tolerances versus relative cost for primary mirror of UV imager (base cost = 100)

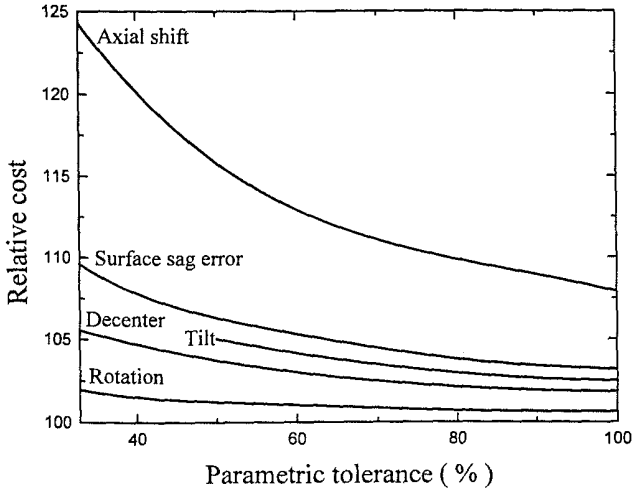

Fig. 14 Parameter tolerances versus relative cost for secondary mirror of UV imager (base cost = 100)

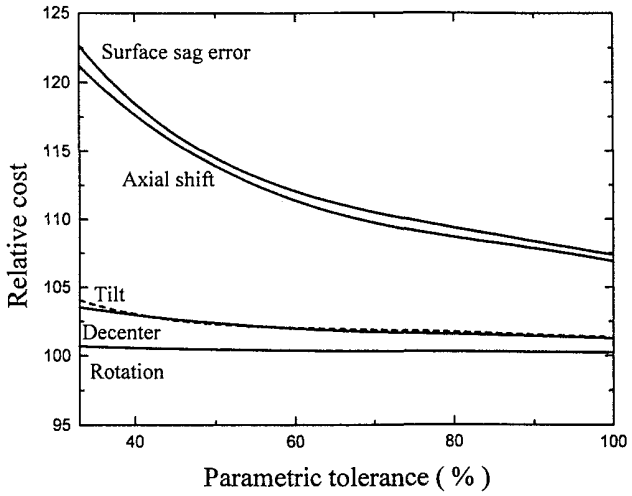

Fig. 15 Parameter tolerances versus relative cost for tertiary mirror of UV imager (base cost = 100)

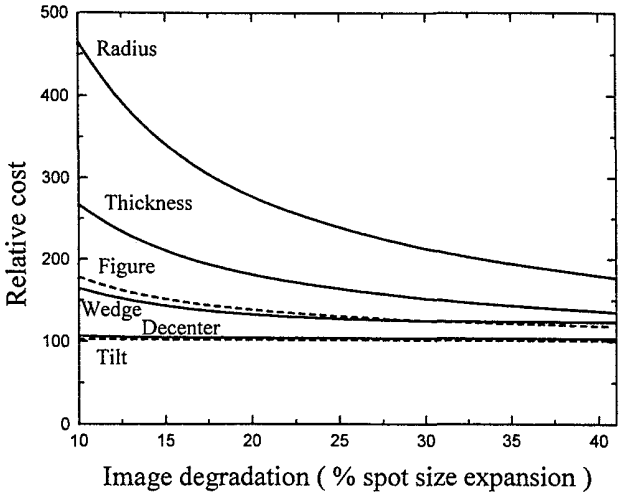

Fig. 16 Spot expansion versus relative cost for afocal telescope objective (base cost = 100).

Acknowledgments

The authors express their gratitude to the staff of the Center for Applied Optics and Optical Aeronomy Laboratory of the University of Alabama in Huntsville and the staff of NASA Marshall Space Flight Center for their technical contributions. The third author would like to thank Central Scientific Instruments Organisation, Chandigarh, India, and the Academy for Educational Development, Washington, D.C., for a fellowship provided to support this work.

References

1 G E Weise, Ed , *Selected Papers on Optical Toleranc ing,* SPIE Milestone Series **MS 36** (1991)
2 D. G. Torr, M R Torr, M Zukic, J F Spann, and R B Johnson, "Ultraviolet imager for the International Terrestrial Physics Mission," *Opt Eng* **32**(12), 3060–3068 (1993)

Table 4 Parameter sensitivities of afocal telescope objective and eyepiece with image degradation

Parameters		41%	30%	20%	10%
Radius (fringes))	obj	1 30	0 89	0 57	0.27
	epc	3 62	2 83	1 94	0 97
Irregularity (fringes)	obj	1 39	1 01	0 66	0 32
	epc	2 32	2 14	1 78	1 06
Thickness (microns)	obj	35 91	24 59	15 68	7 57
	epc	121 81	115 90	102 90	68 65
Decenter (microns)	obj	94 93	92.95	80 94	47 67
	epc	95 29	93 85	82 63	49.33
Wedge (microns)	obj	1 07	1 01	0 77	0 39
	epc	3 73	3 53	2 79	1 45
Tilt (arc minutes)	obj	3 11	2 80	2 25	1 28
	epc	5 50	4 53	3 26	1 62

Table 5 Cost escalation with spot expansion percentage for system parameters of afocal telescope objective and eyepiece (base cost = 100)

Parameters		Image degradation			
		41%	30%	20%	10%
Radius	obj	176 90	212 30	276 00	464 80
	epc	127 00	135 40	151 50	203 40
Surface Irregularity	obj	118 00	124 80	137 90	178 10
	epc	110 80	111 70	114 00	123 60
Thickness	obj	135 20	151 40	180 60	267 00
	epc	110 40	110 90	112 30	118 40
Decenter	obj	103 30	103 40	103 90	106 60
	epc	103 30	103 40	103 80	106 40
Wedge	obj	123 40	124 60	132 20	164 40
	epc	106 70	107 10	108 90	117 20
Tilt	obj	101 05	101 07	101 44	102 55
	epc	101 13	101 37	101 91	103 72

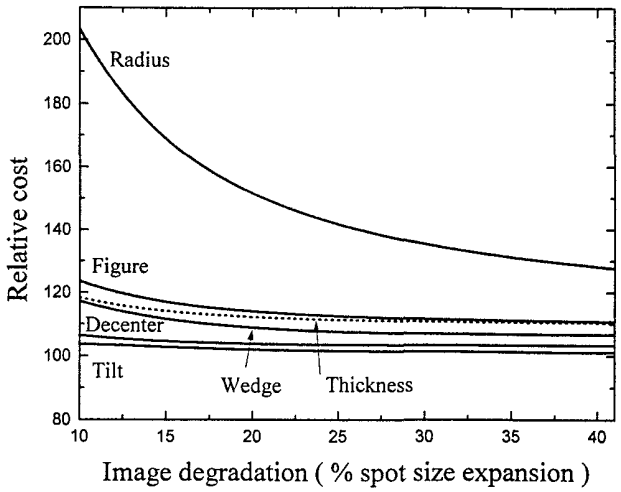

Fig. 17 Spot expansion versus relative cost for afocal telescope eyepiece (base cost = 100).

3. J P Starke and C M Wise, "Modulation-transfer-function based optical sensitivity and tolerancing programs," *Appl Opt* **19**(11), 1768–1772 (1980)
4 M P Rimmer, "A tolerance procedure based on modulation transfer function (MTF)," in *International Conference on Computer-Aided Optical Design, Proc SPIE* **147,** 66–70 (1978)
5 C S. Williams and O A Becklund, *Introduction to the Optical Transfer Function,* Chapter 6, pp 181–210, Wiley, New York (1989)
6 R R Willey, "The impact of tight tolerances and other factors on the cost of optical components," in *Proc SPIE* **518,** 106–111 (1984)
7 R R Willey and R E Parks, "Optical fundamentals," Chapter 1 in *Handbook of Optomechanical Engineering,* A. Ahmad, Ed , CRC Press (to be published)

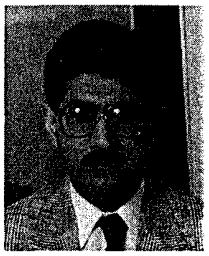

Anees Ahmad is a senior research scientist at the Center for Applied Optics, University of Alabama, Huntsville, AL His research interests include optomechanical design and fabrication of ultralightweight and high-performance photonic systems for commercial space, and military applications He is also involved in the modeling and virtual prototyping of complex optical systems, and the development of knowledge-based expert systems for computer-aided optomechanics design He has several publications and patents in various areas of optomechanical engineering He received his PhD in mechanical engineering from the University of Houston, Texas

Chen Feng is a research scientist in the Center for Applied Optics He has a broad range of experience in lens design, optical system engineering, tolerance analysis, and thermal and structural analysis He has designed and analyzed various electro-optical systems for NASA, the Army, and commercial applications. His recent achievements include optical design of a UV imager and an IR collimator, tolerance analysis of an astronomical spectral camera, and thermal and structural analysis of a lightweight optical testing system Dr. Feng has a BS in mechanical engineering from Shanghai Maritime Institute in China, and an MS and PhD in electro-optics from the Chinese Academy of Sciences

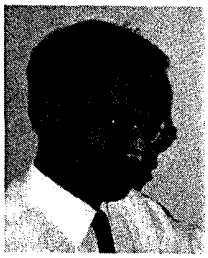

RamaGopal V. Sarepaka received his BSc (physics) degree from Andhra University, India, in 1975, his MSc (physics) from South Gujarat University, India, in 1978, his MTech (applied optics) and PhD from Indian Institute of Technology, Delhi, India, in 1980 and 1989, respectively Since 1983, he has been working as a research scientist with the Optical System Design & Development Division of the Central Scientific Instruments Organisation, Chandigarh, India. Since February 1994, he is working at the Center for Applied Optics, University of Alabama in Huntsville under the Indo-U S. Science and Technology Fellowship Program. His research interests include optical system design and development and related software development He is a member of the Optical Society of India and the Instrument Society of India